





Alterations of the Primary Cilia Gene *SPAG17* and *SOX9* Locus Noncoding RNAs Identified by RNA-Sequencing Analysis in Patients With Systemic Sclerosis

Elisha D. O. Roberson,¹  Mary Carns,² Li Cao,³ Kathleen Aren,² Isaac A. Goldberg,²  David J. Morales-Heil,³ Benjamin D. Korman,²  John P. Atkinson,³  and John Varga⁴

Objective. Systemic sclerosis (SSc) is characterized by immune activation, vasculopathy, and unresolving fibrosis in the skin, lungs, and other organs. We performed RNA-sequencing analysis on skin biopsy samples and peripheral blood mononuclear cells (PBMCs) from SSc patients and unaffected controls to better understand the pathogenesis of SSc.

Methods. We analyzed these data 1) to test for case/control differences and 2) to identify genes whose expression levels correlate with SSc severity as measured by local skin score, modified Rodnan skin thickness score (MRSS), forced vital capacity (FVC), or diffusing capacity for carbon monoxide (DL_{CO}).

Results. We found that PBMCs from SSc patients showed a strong type I interferon signature. This signal was found to be replicated in the skin, with additional signals for increased extracellular matrix (ECM) genes, classical complement pathway activation, and the presence of B cells. Notably, we observed a marked decrease in the expression of *SPAG17*, a cilia component, in SSc skin. We identified genes that correlated with the MRSS, DL_{CO}, and FVC in SSc PBMCs and skin using weighted gene coexpression network analysis. These genes were largely distinct from the case/control differentially expressed genes. In PBMCs, type I interferon signatures negatively correlated with the DL_{CO}. In SSc skin, ECM gene expression positively correlated with the MRSS. Network analysis of SSc skin genes that correlated with clinical features identified the noncoding RNAs *SOX9-AS1* and *ROCR*, both near the *SOX9* locus, as highly connected, “hub-like” genes in the network.

Conclusion. These results identify noncoding RNAs and *SPAG17* as novel factors potentially implicated in the pathogenesis of SSc.

INTRODUCTION

Systemic sclerosis (SSc) is a complex orphan disease characterized by autoantibodies, vasculopathy of small vessels, and synchronous/unresolving fibrosis in multiple organs (1,2).

There is substantial patient-to-patient heterogeneity in clinical features, disease severity, and the rates of progression. Currently, there are few effective treatments for SSc. Moreover, there is a lack of molecular biomarkers that reliably predict clinical course, reflect disease activity, or identify rational therapeutic targets (3).

The research presented herein represents the views of the authors and does not necessarily reflect the views of the NIH.

Supported in part by the Washington University Center for High Performance Computing (grant S10-OD-018091). Sequencing data were generated at the Genome Technology Access Center at the McDonnell Genome Institute (GTAC@MGI) of Washington University. GTAC was supported by the Sitman Cancer Center (grant P30-CA91842) and the Institute of Clinical and Translational Sciences (ICTS) (grant UL1-TR-000448). Dr. Roberson's work was supported by the National Institute of Arthritis and Musculoskeletal and Skin Diseases (NIAMS) Rheumatic Disease Core Center, NIH (grant P30-AR-048335), the NIAMS Rheumatic Diseases Research Resource-based Center, NIH (grant P30-AR-073752), and the ICTS of Washington University in St. Louis (grant UL1-TR-000448). Dr. Cao's work was supported by the NIAMS Rheumatic Disease Core Center, NIH, (grant P30-AR-048335). Dr. Morales-Heil's work was supported by an NIH training grant (T32-AR-007279-36). Dr. Atkinson's work was supported by the NIAMS Rheumatic Disease Core Center, NIH (grant P30-AR-048335), and the ICTS of Washington University in St. Louis (grant UL1-TR-000448). Dr. Varga's work was supported by the Northwestern University Clinical and Translational Sciences Institute (grant UL1-TR-000150).

¹Elisha D. O. Roberson, PhD: Department of Medicine, Division of Rheumatology, and Department of Genetics, Washington University, St. Louis, Missouri; ²Mary Carns, MS, Kathleen Aren, MPH, Isaac A. Goldberg, BA, Benjamin D. Korman, MD: Scleroderma Program, Feinberg School of Medicine, Northwestern University, Chicago, Illinois; ³Li Cao, MD, David J. Morales-Heil, PhD, John P. Atkinson, MD: Department of Medicine, Division of Rheumatology, Washington University, St. Louis, Missouri; ⁴John Varga, MD (current address: Division of Rheumatology, University of Michigan, Ann Arbor): Scleroderma Program, Feinberg School of Medicine, Northwestern University, Chicago, Illinois, and Department of Internal Medicine, Division of Rheumatology, University of Michigan, Ann Arbor.

Author disclosures are available at <https://onlinelibrary.wiley.com/action/downloadSupplement?doi=10.1002%2Fart.42281&file=art42281-sup-0001-Disclosureform.pdf>.

Address correspondence via email to Elisha D. O. Roberson, PhD, at eroberson@wustl.edu; or to John Varga, MD, at vargaj@med.umich.edu.

Submitted for publication January 6, 2022; accepted in revised form June 23, 2022.

One approach to improve our understanding of the evolution and progression of the disease is through transcriptomics. Previous primary and secondary analyses of transcriptome data in SSc used microarray, bulk RNA sequencing (RNA-Seq), and single-cell RNA-Seq approaches. These studies revealed molecular heterogeneity among individual transcriptomes, increased type I interferon signaling, potential molecular subtypes, and altered cell populations in the skin (4–13). We sought to further clarify molecular disruptions in SSc, to find correlations with clinical measures of disease activity, and to determine if expression–trait correlation gene sets overlap with the case/control differential expression gene sets. We used prospective collection of skin and peripheral blood mononuclear cell (PBMC) samples from unaffected control subjects and patients with SSc followed by bulk RNA-Seq. At each visit, disease severity was assessed by the local skin score, modified Rodnan skin thickness score (MRSS), and pulmonary function testing. For RNA-Seq, we used a ribosomal depletion method to permit the detection of both nascent and mature messenger RNA, along with noncoding RNAs lacking a poly(A) tail. This method may be more sensitive for genes with low expression levels or short half-lives than poly(A)-based RNA-Seq methods, enabling us to identify potentially overlooked contributors to SSc. These methodologies allowed us to examine categorical differences between SSc patients and unaffected controls, as well as to identify genes whose expression is correlated with alterations in established clinical parameters of disease progression.

PATIENTS AND METHODS

Clinical assessment. We completed standardized evaluations to establish SSc diagnosis, as well as the presence/severity of organ involvement, as previously described (14,15). We determined MRSS and local (forearm) skin scores at each visit. High-resolution computed tomography of the chest, echocardiography, and pulmonary function testing were performed as standard of care (16). At each research visit, we collected PBMCs and 2 skin punch biopsy samples (stabilized in RNA later).

Genomics methods and analysis. Detailed methods can be found in the Supplementary Methods on the *Arthritis & Rheumatology* website, available at <http://onlinelibrary.wiley.com/doi/10.1002/art.42281>. Briefly, we used RNA extracted from the blood and PBMC samples (miRNeasy minikit no. 217004) to create stranded, ribosomal depletion libraries (Takara/Clontech product no. 634876). We trimmed raw sequencing data with Cutadapt, aligned to the human genome with RNaSTAR, and counted read-pairs per gene with featureCounts (17–19). We then calculated differential expression with DESeq2 and pathway enrichment with gProfiler, and we performed network analyses with weighted gene coexpression network analysis (WGCNA) (20–22).

Data availability. The data used in the analysis, such as gene counts used for DESeq2 and demographic information per sample, are available from FigShare at https://figshare.com/projects/2021_Roberson_lab_systemic_sclerosis_transcriptome_data/118698. The code used for data analysis is available as a repository on GitHub at https://github.com/RobersonLab/2021_ssc_rnaseq. These were prospectively collected samples for controlled data access. FASTQ files are available for general research use in dbGAP accession phs002902.v1.p1.

RESULTS

Study cohort and demographics. Patients with SSc (n = 21) were recruited from the Northwestern Scleroderma Clinic and fulfilled the 2013 American College of Rheumatology/EULAR classification criteria for SSc (1). These patients were further classified as having limited cutaneous SSc (lcSSc; n = 5), diffuse cutaneous SSc (dcSSc; n = 14), SSc without scleroderma (sine scleroderma SSc; n = 1), or very early diagnosis of SSc (VEDOSS; n = 1). Controls were volunteers with no history of an autoimmune or inflammatory disease (n = 14). At each study visit, we obtained whole blood samples and 2 skin punch biopsy samples measuring 3 mm. We also conducted pulmonary function tests, and the same observer assessed the MRSS and local skin score. Seven patients with dcSSc, 2 with lcSSc, and 1 individual with sine scleroderma SSc volunteered to provide a second set of whole blood and skin biopsy samples and to undergo additional pulmonary function testing.

For group-wise demographic summaries, we included unaffected controls and patients with either lcSSc or dcSSc (n = 19) (Table 1). Controls were younger than SSc patients. Within the SSc cohort, the lcSSc and dcSSc subsets were balanced for patient age and disease duration (Table 2). There were

Table 1. Demographic characteristics of systemic sclerosis (SSc) patients and unaffected controls*

	Controls (n = 14)	SSc patients (n = 19)
Age, mean ± SD years	32.6 ± 10.8	49.7 ± 11.4
Female	9 (64.3)	15 (78.9)
Race/ethnicity		
Asian	0 (0.0)	2 (10.5)
Black	3 (21.4)	2 (10.5)
Hispanic	5 (35.7)	0 (0.0)
White	6 (42.9)	15 (78.9)

* Except where indicated otherwise, values are the number (%) of patients. Controls were individuals without a self-reported history of autoimmune disease. SSc patients met the 2013 American College of Rheumatology/EULAR classification criteria for SSc. The unaffected controls were significantly younger than the SSc patients ($P < 0.05$ by Student's 2-tailed t -test), but the distribution of female patients was balanced between the groups ($P > 0.05$ by Fisher's exact test). The participants in both the control and SSc cohorts were predominantly White, and the other racial/ethnic backgrounds were significantly different between the 2 cohorts ($P < 0.05$ by Fisher's exact test).

Table 2. Demographic characteristics and antibody staining patterns of patients with diffuse cutaneous systemic sclerosis (dcSSc) and patients with limited cutaneous SSc (lcSSc)*

	dcSSc (n = 14)	lcSSc (n = 5)
Age, mean ± SD years	49.7 ± 11.7	49.8 ± 11.9
Female	13 (92.9)	2 (40.0)
Duration of disease, mean ± SD months	42.7 ± 33.2	36.2 ± 22.8
MRSS, mean ± SD	24.1 ± 10.2	8.8 ± 5.0
Forearm MRSS, mean ± SD	1.9 ± 0.9	0.8 ± 0.8
BMI, mean ± SD	26.7 ± 5.5	29.5 ± 6.3
FVC, mean ± SD†	75.1 ± 15.6	82.6 ± 12.5
Corrected DLco, mean ± SD†	66.2 ± 20.8	80.0 ± 17.4
TLC, mean ± SD†	85.6 ± 17.2	85.8 ± 11.7
Race/ethnicity		
Asian	1 (7.1)	1 (20.0)
Black	2 (14.3)	0 (0.0)
Hispanic	0 (0.0)	0 (0.0)
White	11 (78.6)	4 (80.0)
Immunofluorescence pattern‡		
Centromere	1 (8.3)	2 (40.0)
Homogeneous	3 (25.0)	0 (0.0)
Nucleolar	4 (33.3)	1 (20.0)
Speckled	7 (58.3)	3 (60.0)

* Except where indicated otherwise, values are the number (%) of patients. The modified Rodnan skin thickness score (MRSS), body mass index (BMI), forced vital capacity (FVC), diffusing capacity for carbon monoxide (DLco), and total lung capacity (TLC) were determined at repeat visits. For each individual, we used the “worst” observed value as the representative value.

† Lung function parameters were calculated as percent estimated maximum for age and sex.

‡ Immunofluorescence data were only available for 12 of the 14 individuals with dcSSc, and percentages were calculated based on this availability.

more women in the dcSSc subset than in the lcSSc subset, while self-declared ethnicity was similar between the 2 groups. The medications that patients were being treated with at sample collection are listed in Supplementary Table 1 (<http://onlinelibrary.wiley.com/doi/10.1002/art.42281>).

Evidence of increased type I interferon signaling by SSc PBMCs. We sought to characterize gene expression changes in PBMCs of SSc patients since collection of PBMCs is minimally invasive. For cases, we only included baseline lcSSc and dcSSc samples to avoid bias toward individuals sampled more than once. There were 147 genes with decreased expression levels (113 genes with at least -1.5 -fold decreased expression) and 100 genes with increased expression levels (61 genes with at least 1.5 -fold increased expression) in the PBMCs of SSc patients compared to the PBMCs of unaffected controls (Figure 1A and Supplementary Table 2, <http://onlinelibrary.wiley.com/doi/10.1002/art.42281>). The genes with the most significantly decreased expression levels included *GALNTL6* (fold change -4.09), *GPM6A* (fold change -3.98), *SLC4A10* (fold change -3.33), and *COL4A3* (fold change -4.36). The most

consistently enriched pathways among genes with decreased expression levels in SSc patients were collagen pathways due to decreases in *COL4A3* and *COL4A4* (Figure 1B and Supplementary Table 3, <http://onlinelibrary.wiley.com/doi/10.1002/art.42281>).

Genes with significantly increased expression levels in the PBMCs of SSc patients compared to unaffected controls included *FAM13A* (fold change 2.49), *E2F2* (fold change 2.28), *MYOF* (fold change 1.83), and *TMEM178B* (fold change 1.36). Single-nucleotide polymorphisms in *FAM13A* are associated with an increased risk of pulmonary fibrosis (23) and liver cirrhosis (24). We tested the genes with increased expression levels in SSc PBMCs for pathway enrichment (Figure 1C and Supplementary Table 4, <http://onlinelibrary.wiley.com/doi/10.1002/art.42281>). The most significant pathways were related to type I interferon activity, including interferon- α /interferon- β and type I interferon signaling categories. Target genes of interferon regulatory factor 5 (IRF-5) and IRF-9 transcription factors were significantly enriched in the genes with increased expression levels. *IRF5* is highly expressed in classically activated (M1-polarized) human macrophages (25). M1-like macrophage signatures have been found to be highly prevalent in the skin of SSc patients (10).

Previous studies have identified similarly increased expression of type I interferon-stimulated genes in the PBMCs of SSc patients as well as in the skin (26,27). It is also interesting to consider whether some of these signatures, including the increase in IRF-5 and its known high expression in M1-polarized macrophages, indicate a specific role for this macrophage subpopulation in SSc.

Evidence of substantial immune activation, increased complement component expression, and loss of ciliary protein *SPAG17* in SSc skin.

Procurement of PBMCs is minimally invasive but may not reflect the molecular biology of affected tissues. Evaluation of the skin tissue may therefore provide more insight into the molecular defects in the setting of SSc. Expression levels of 526 genes were significantly decreased (226 genes with at least -1.5 -fold decreased expression) and expression levels of 1,200 genes were increased (816 genes with at least 1.5 -fold increased expression) (Figure 2A and Supplementary Table 5, <http://onlinelibrary.wiley.com/doi/10.1002/art.42281>) in the skin biopsy samples of SSc patients compared to the skin biopsy samples of unaffected controls. These results help highlight the advantage of studying tissue affected by SSc.

The most significantly altered gene in the entire study was *SPAG17*, which was decreased in SSc skin samples compared to unaffected control skin samples (fold change -4.67 ; adjusted $P = 3.22 \times 10^{-12}$). To our knowledge, this gene had not been previously associated with differential expression in SSc skin. The expression level of *SPAG17* is relatively low, and previous studies using hybridization microarrays may not have been

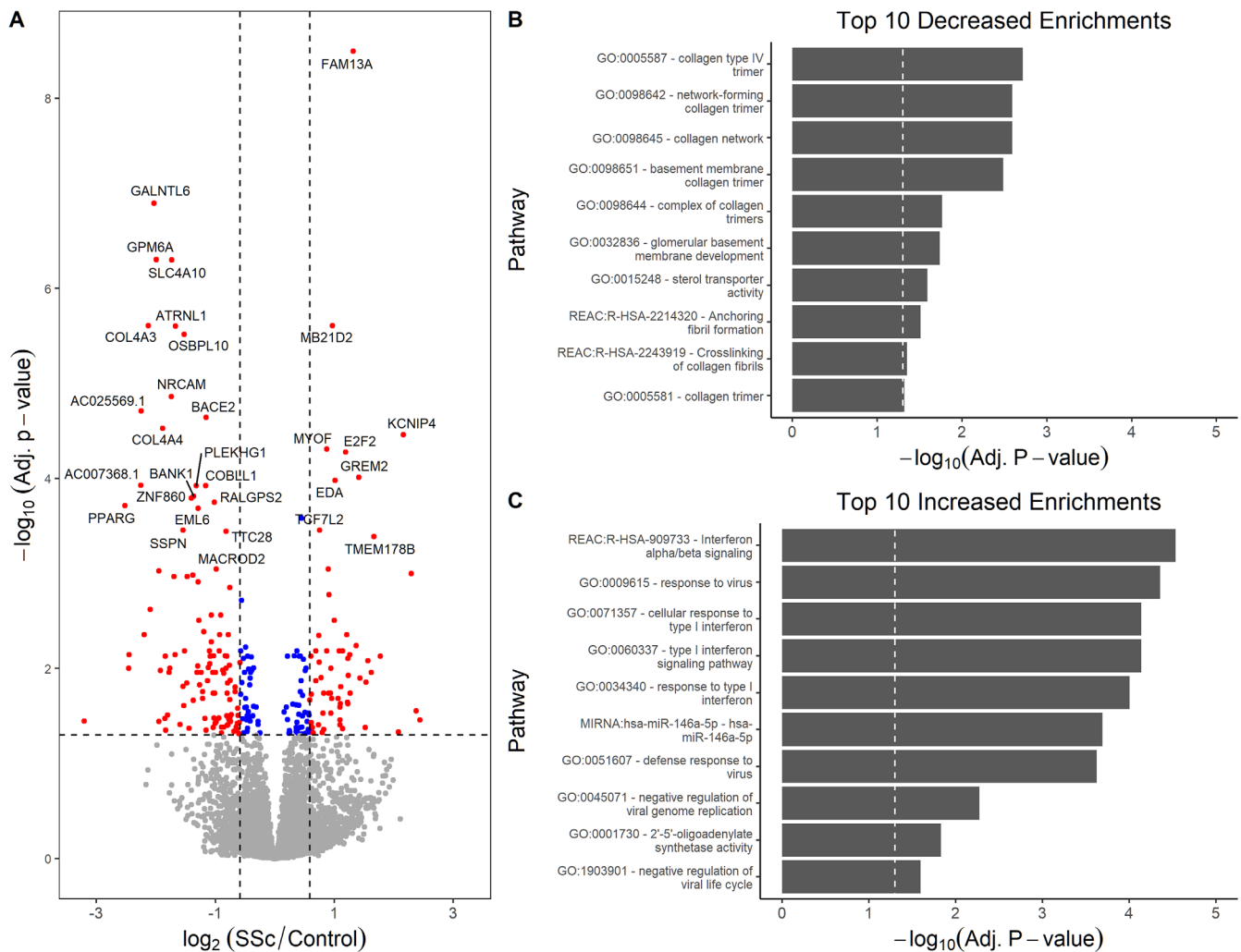


Figure 1. Strong enrichment for the type I interferon signaling pathway in systemic sclerosis (SSc) peripheral blood mononuclear cells (PBMCs). **A**, Standard volcano plots showing the effect size in SSc patients relative to unaffected controls (fold change on a \log_2 scale) and the P values for differences in SSc patients vs. controls (on a \log_{10} scale). Vertical dashed lines show the cutoff value for a 1.5-fold change defining up- or down-regulated genes. Horizontal dashed line indicates the adjusted significance threshold of 0.05. **B** and **C**, Bar graphs showing pathways enriched for genes that displayed decreased (**B**) or increased (**C**) expression in PBMCs from SSc patients relative to unaffected controls. Genes with at least a 1.5-fold change in expression were tested, with the predominant signal being increased type I interferon signaling. Some of the most significant enrichments included collagen and sterol transporter. The vertical dashed line shows the adjusted threshold of significance ($P = 0.05$). Color figure can be viewed in the online issue, which is available at <http://onlinelibrary.wiley.com/doi/10.1002/art.42281/abstract>.

sensitive enough to detect its expression against background fluorescence. Low expression level might also cause *SPAG17* to be filtered out of some RNA-Seq studies. *SPAG17* protein is required for the function of primary cilia and male fertility (28). Mice deficient in *Spag17* have bone abnormalities such as decreased femur length and disrupted femur morphology (29). The role of *SPAG17* in skin and immune cells is not particularly clear, though as part of the primary cilia it could be involved in signaling. Decreased expression levels of *SPAG17* may be present without any appreciable evidence of skin fibrosis, as skin samples of patients with sine scleroderma SSc had decreased *SPAG17* expression levels that were comparable to the levels in skin samples from patients with lcSSc or those with dcSSc (Supplementary Figure 2, <http://onlinelibrary.wiley.com/doi/10.1002/art.42281>).

The similarity of the skin transcriptomes from patients with sine scleroderma SSc, patients with lcSSc, and patients with dcSSc was also shown by principal components analysis of the top case/control differentially expressed genes (Supplementary Methods and Supplementary Figure 4, <http://onlinelibrary.wiley.com/doi/10.1002/art.42281>).

Another gene with significantly decreased expression levels was *LGR5* (fold change -2.70). *LGR5* is a member of the G protein-coupled receptor family that is an important target and modulator of Wnt/ β -catenin signaling. *LGR5* expression is a marker for intestinal villi tip telocytes in mice that maintain the correct differentiation gradient on the villus axis via noncanonical Wnt signaling (30). Dermal telocytes are reduced in the fibrotic skin and internal organs of individuals with SSc (31,32). If these dermal

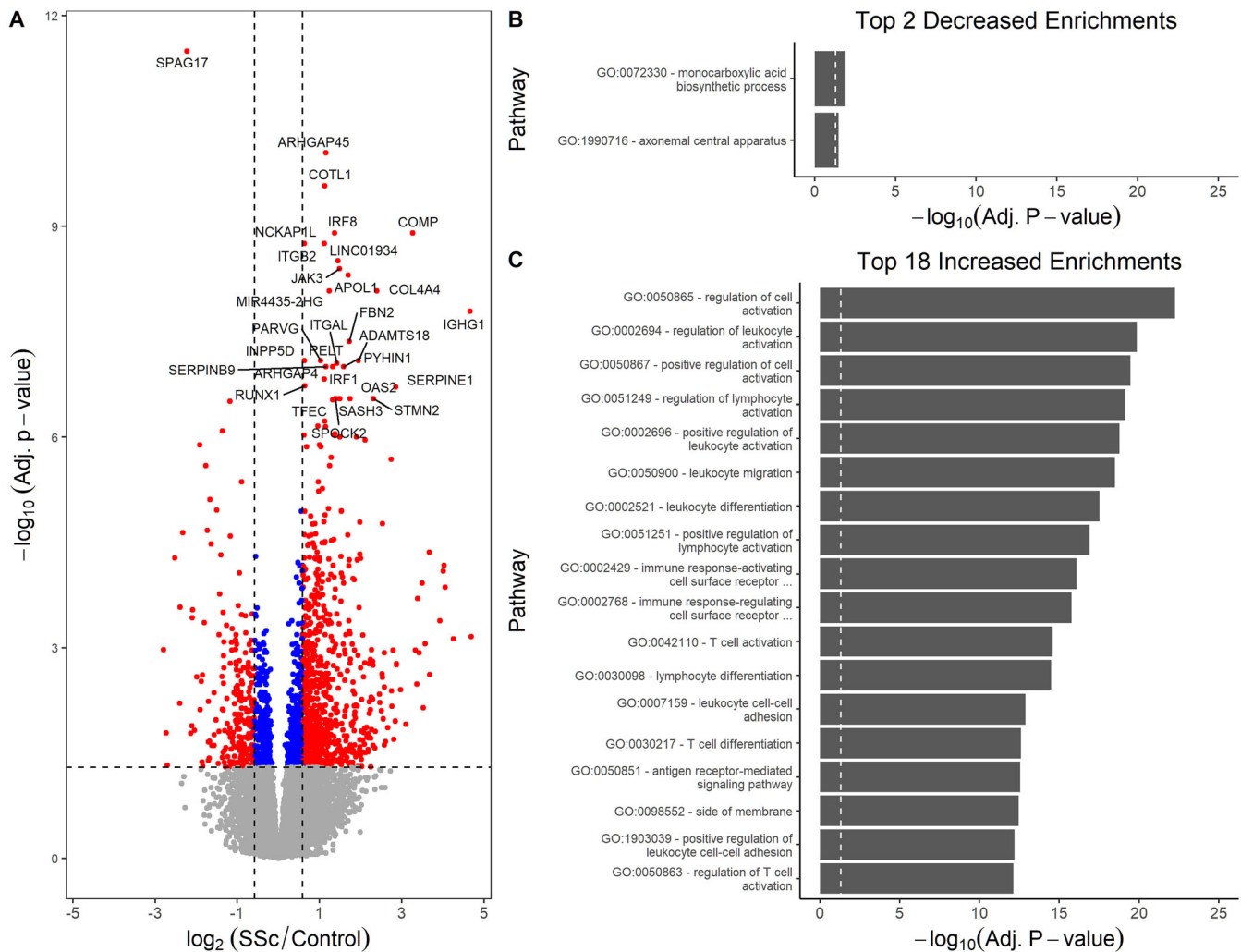


Figure 2. Decreased expression of primary cilia protein SPAG17 and increased immune activation in SSc skin. **A**, Standard volcano plot showing the effect size in SSc patients relative to unaffected controls (fold change on a \log_2 scale) and the P values for differences in SSc patients vs. controls (on a \log_{10} scale). Vertical dashed lines show the cutoff value for a 1.5-fold change defining up- or down-regulated genes. Horizontal dashed line indicates the adjusted significance threshold of 0.05. More genes were significantly increased in SSc skin than were significantly decreased. **B** and **C**, Bar graphs showing pathways enriched for genes that displayed decreased (**B**) or increased (**C**) expression in skin from SSc patients relative to unaffected controls. Genes with at least a 1.5-fold change in expression were tested, with the predominant enrichments for genes related to immune cell activation, indicating the migration of immune cells into the skin. The vertical dashed line shows the adjusted threshold of significance ($P = 0.05$). Color figure can be viewed in the online issue, which is available at <http://onlinelibrary.wiley.com/doi/10.1002/art.42281/abstract>.

telocytes also help to coordinate differentiation and/or signaling in the skin, their loss (perhaps detected by the reduction of *LGR5*) may directly contribute to the development of SSc fibrosis. Only 2 known pathways were enriched among genes with decreased expression levels (Figure 2B and Supplementary Table 6, <http://onlinelibrary.wiley.com/doi/10.1002/art.42281>): monocarboxylic acid biosynthesis and axonemal central apparatus.

Genes with increased expression levels in SSc patients included *ARHGAP45* (fold change 2.22), *COTL1* (fold change 2.18), *IRF8* (fold change 2.57), and *COMP* (fold change 9.63). The extensive list of genes with increased expression levels in SSc skin would allow us to posit interesting hypotheses for almost any one of them. We therefore chose to check these genes for the

enrichment of known molecular pathways as well. We found a total of 366 significant enrichments (Figure 2C and Supplementary Table 7, <http://onlinelibrary.wiley.com/doi/10.1002/art.42281>), including enrichment for targets of the transcription factors IRF2, IRF4, IRF5, IRF7, IRF8, IRF9, and ISGF3. The RNA expression levels of transcription factors *IRF1* (fold change 2.65), *IRF5* (fold change 1.48), *IRF7* (fold change 1.99), and *IRF8* (fold change 2.57) were all significantly increased in the skin of SSc patients as well.

Some of the enriched pathways had functions that involved variations on similar themes, such as immune cell adhesion, migration, and differentiation, B cell activation and proliferation, extracellular matrix deposition, and classical antibody-mediated

complement activation. The complement theme was mainly due to increased expression levels of complement genes (including *C1QB*, *CR1*, *C5AR1*, and *C7*) and immunoglobulins. Complement activation usually leads to the assembly of the membrane-attack complex (MAC) that can insert into membranes and lyse cells. The MAC is composed of complement proteins C5b, C6, C7, C8, and C9. MAC fragments are deposited in the dermal vasculature of SSc patients, supporting a role for antibody-induced complement activation in SSc vasculopathy (33). These data suggest that aberrant activation of complement may partially mediate cutaneous tissue damage in SSc.

WGCNA findings of correlations between gene expression and severity of skin fibrosis and changes in lung function.

Group-wise gene expression analysis categorizes samples as test (SSc) or reference (control). This is a reasonable way to determine the general features of a trait, but it ignores the heterogeneity of phenotypes within the trait. SSc in particular has substantial clinical heterogeneity. We used WGCNA to assess correlations between gene expression and severity of skin fibrosis (MRSS and forearm local skin scores) or changes in lung function (forced vital capacity [FVC] and DL_{CO}). This approach is somewhat different from that used in other studies, in which correlations between gene expression array findings and the MRSS score in the skin have been assessed or correlations between gene expression levels in lung biopsy samples and the severity of lung disease have been assessed (34–36). We chose to test both skin and lung phenotypes and used paired samples from PBMCs and skin for each individual. We included all SSc samples for which there was a matching MRSS, FVC, or DL_{CO} measurement for the visit (i.e., follow-ups were included as separate measurements). The tallies of positive and negative correlations by tissue are listed in Supplementary Table 8 (<http://onlinelibrary.wiley.com/doi/10.1002/art.42281>).

For PBMCs, there were significant correlations between gene expression and DL_{CO}, forearm skin score, and MRSS (Supplementary Tables 9, 10, and 11, respectively, <http://onlinelibrary.wiley.com/doi/10.1002/art.42281>). The genes negatively correlated with DL_{CO} were enriched for type I interferon signaling and proteasomal antigen processing/presentation (Supplementary Table 12, <http://onlinelibrary.wiley.com/doi/10.1002/art.42281>). The PBMC genes that positively correlated with DL_{CO} were only enriched for targets of microRNA hsa-miR-6082 (*DTWD2*, *FXN*, and *ZFP30*; Supplementary Table 13, <http://onlinelibrary.wiley.com/doi/10.1002/art.42281>).

Correlations between gene expression levels and the forearm-specific skin score (Supplementary Table 10) were more difficult to interpret. The negative correlations did not show any pathway enrichments. Positive correlations were only enriched for the phosphoribosylformylglycinamide synthase pathway, but it was due to a single gene (*PFAS*; Supplementary Table 14, <http://onlinelibrary.wiley.com/doi/10.1002/art.42281>).

There were also correlations between PBMC gene expression and the MRSS score (Supplementary Table 10). Genes negatively correlated with the MRSS score were enriched for pathways associated with protein folding, unfolded proteins, and endoplasmic reticulum stress (Supplementary Table 15, <http://onlinelibrary.wiley.com/doi/10.1002/art.42281>). There were a few pathways associated with positively correlated genes, including some related to Wnt signaling regulation and mitochondrial functions (Supplementary Table 16, <http://onlinelibrary.wiley.com/doi/10.1002/art.42281>).

One might assume that the differentially expressed genes in case/control gene expression studies may also be the key genes and pathways that drive progression and therefore may correlate with disease severity. This does not appear to be the case for SSc PBMCs, as most of the genes with significant correlations to disease severity were not detected in the case/control analysis (Supplementary Figure 6, <http://onlinelibrary.wiley.com/doi/10.1002/art.42281>).

The SSc skin transcriptomes had significant correlations with the DL_{CO}, FVC, and MRSS (Supplementary Tables 17, 18, and 19, respectively, <http://onlinelibrary.wiley.com/doi/10.1002/art.42281>). In evaluating correlations with the DL_{CO}, there were many negative correlations with expression of ribosomal proteins, leading to enrichment of pathways related to ribosome function (Supplementary Table 20, <http://onlinelibrary.wiley.com/doi/10.1002/art.42281>). SSc skin genes that positively correlated with the DL_{CO} did not follow a consistent pattern of enrichment (Supplementary Table 21, <http://onlinelibrary.wiley.com/doi/10.1002/art.42281>). Genes that were negatively correlated with the FVC were enriched for sterol/cholesterol biosynthesis and α -linolenic/linolenic acid metabolism pathways (Supplementary Table 22, <http://onlinelibrary.wiley.com/doi/10.1002/art.42281>). Genes that were positively correlated with the FVC did not have any significant pathway enrichment.

Genes whose expression levels showed a negative correlation with the MRSS in the skin were enriched in cell fate and synaptic functions (Supplementary Table 23, <http://onlinelibrary.wiley.com/doi/10.1002/art.42281>). Genes with expression levels that positively correlated with the MRSS were enriched for extracellular matrix functions (Supplementary Table 24, <http://onlinelibrary.wiley.com/doi/10.1002/art.42281>). This is a nice confirmation, as increasing MRSS is expected to indicate increasing fibrosis, secondary to increased matrix deposition.

Similar to what we observed in PBMCs, there is little overlap between the genes differentially expressed in SSc skin and skin genes that correlated with lung function or skin fibrosis parameters (Supplementary Figure 7, <http://onlinelibrary.wiley.com/doi/10.1002/art.42281>). Overall, 90% of the differentially expressed genes did not correlate with any clinical parameters, and 93% of the clinical trait-associated genes were not differentially expressed. This highlights the disparity between the 2 methods and suggests that novel targets for clinical treatment and

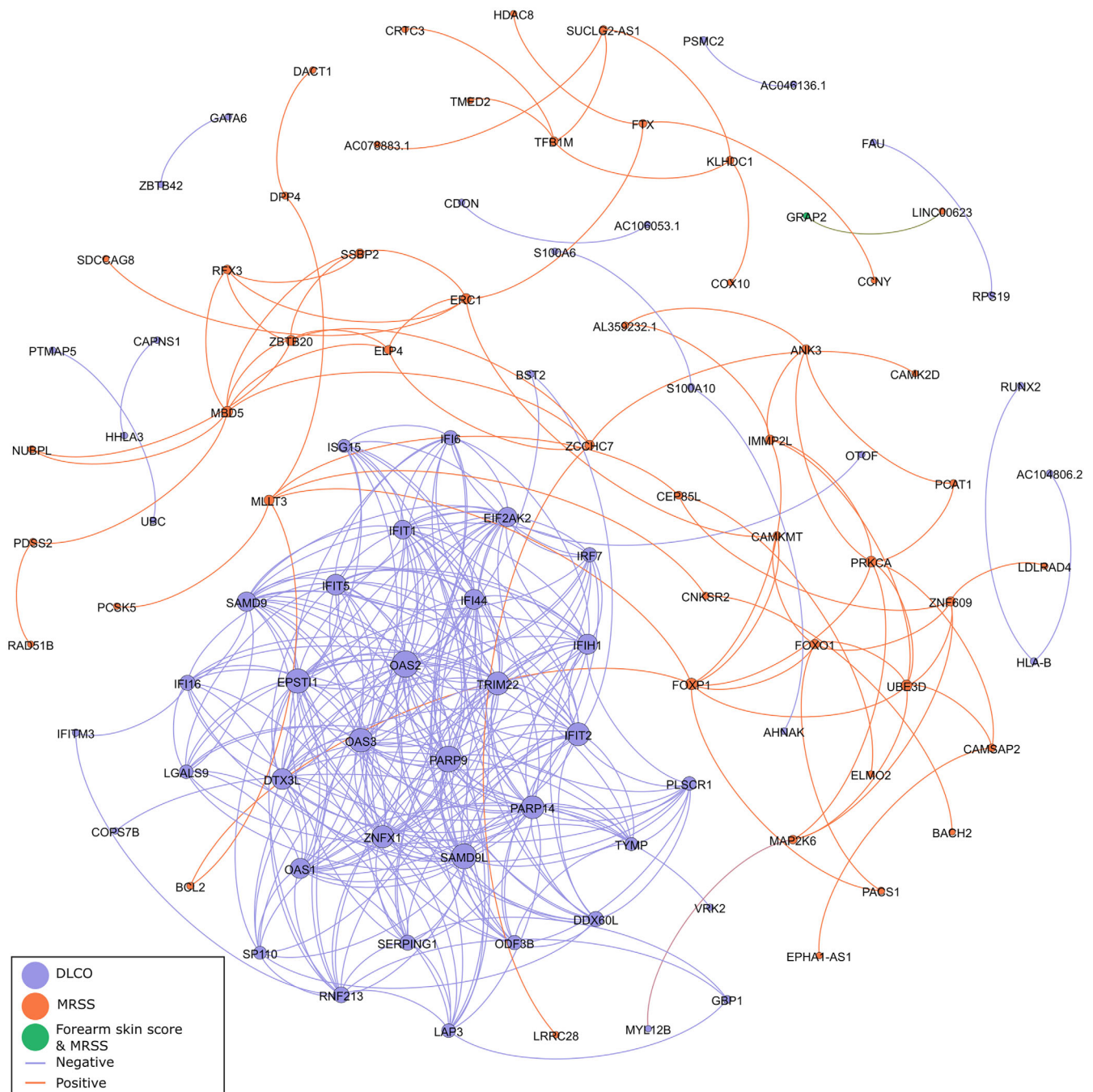


Figure 3. Network diagram of the genes, particularly interferon-responsive genes, most highly connected with at least 1 of the indicated clinical traits in SSc PBMCs. Each node is an individual gene, sized by weighted degree and filled by the trait association. Each edge is color-coded to indicate whether the gene–gene correlation is positive or negative, with a minimum cutoff of 0.80. The interferon-responsive genes, such as *OAS1*, *OAS2*, and *OAS3*, and the gene *IFIT1/2*, were the most highly interconnected in SSc PBMCs. DL_{CO} = diffusing capacity for carbon monoxide; MRSS = modified Rodnan skin thickness score (see Figure 1 for other definitions).

biomarkers may be identified using severity correlation rather than case/control differential gene expression.

Some genes were correlated with the same trait in both skin samples and PBMCs (Supplementary Table 25, <http://onlinelibrary.wiley.com/doi/10.1002/art.42281>). For each gene, we considered the tissues concordant if the direction of effect was the same in each tissue, and discordant if the direction of

effect was opposite. There were only overlaps of gene effects between PBMCs and skin tissue when correlations with the DL_{CO} or MRSS score were assessed. In evaluating correlations with the DL_{CO}, there were 12 concordant genes and 7 discordant genes between tissues. In evaluating correlations with the MRSS, there were 11 concordant genes and 2 discordant genes between tissues. These 2 gene sets are intriguing to consider for further study

as molecular biomarkers of disease activity, regardless of whether the effect is concordant or discordant, as a blood draw sample might be as informative as a skin punch biopsy sample.

We were also interested in whether there are some genes for which expression levels in PBMCs could be as informative as expression levels in skin biopsy samples. A total of 91 genes were differentially expressed in skin samples and PBMCs ($n = 24$) and/or correlated with a clinical trait in both tissues ($n = 69$). We used Pearson's correlation tests with all samples to see if the expression level of these genes correlated between tissues. Among these candidates, 9 genes were significantly correlated between tissues (Supplementary Table 26, <http://onlinelibrary.wiley.com/doi/10.1002/art.42281>). The expression levels of several genes related to interferon activity in PBMCs (*IFI44*, *IF44L*, *OAS1*, *OAS3*, and *RSAD2*) correlated with expression levels in skin samples; therefore, these genes could perhaps be assayed without the need for a skin biopsy as well.

Noncoding RNAs *SOX9-AS1* and *ROCR* as central, highly connected nodes in the SSc skin gene-gene correlation network. Given that we had a list of genes that correlated with different traits and their normalized expression, the next thing we looked at was the gene-gene correlation network. We focused only on genes that significantly correlated with at least 1 clinical trait. Examining the network characteristics can help identify genes that act as signaling hubs or otherwise have coexpression with other members of the network.

After ranking each gene by degree and page rank (measures of network connectedness and centrality), the top-ranked PBMC gene was *OAS2*, with a degree of 29 and page rank of 0.017 (Figure 3 and Supplementary Table 27, <http://onlinelibrary.wiley.com/doi/10.1002/art.42281>). The oligoadenylate synthetases are interferon response genes, which is consistent with the increased type I interferon signaling signatures we found in SSc PBMCs. The 4th highest ranked gene, *EPSTI1*, is linked to macrophage function. It is thought to have a key role in the classical M1 polarization of macrophages, as a murine knockout of *Epsti1* has few M1-polarized macrophages along with a significant expansion of M2-polarized macrophages (37). The top-ranked genes in SSc PBMCs (all genes with a degree of at least 10) are inflammatory genes that correlated with DLCO.

Conversely, the top 41 genes in the SSc skin network (ranked by degree and page rank) all correlated with the MRSS (Figure 4 and Supplementary Table 28, <http://onlinelibrary.wiley.com/doi/10.1002/art.42281>). The top-ranked SSc skin gene was an antisense transcript, *SOX9-AS1* (degree 49; page rank 0.005). This suggests an important advantage of using stranded RNA library kits: with an unstranded kit, it is impossible to tell sense from antisense transcripts if they overlap at the same locus. The protein-coding *SOX9* transcript was correlated with the MRSS as well but had a lower degree of 9. The long noncoding RNA *ROCR* is also a highly connected gene in the SSc skin

network (degree 44; page rank 0.004). It is located in the same genomic locus as *SOX9* and *SOX9-AS1*. It is worth noting that *SPAG17* expression level in SSc skin was negatively correlated with the MRSS (-0.51 correlation). Since *SPAG17* is a low-expression transcript, we were unable to generate a *SPAG17* network to identify coexpressed genes. Therefore, further study is required to understand the genes coexpressed with *SPAG17* in relevant skin cell types, such as fibroblasts.

DISCUSSION

SSc is a complex and progressive inflammatory/fibrotic disease. In the current study, we demonstrated that the sensitivity of RNA-Seq can lead to new discoveries and that applying complementary approaches to the same data can reveal distinct trends. There are advantages to using strand-specific, ribosomal depletion RNA-Seq library kits, such as an increased ability to detect nonpolyadenylated transcripts, an increased sensitivity for nascent and short half-life transcripts, and the ability to distinguish overlapping antisense transcripts. However, one disadvantage is the reduced power for transcript-level discoveries. For our data, focusing only on spliced transcripts would have used only a fraction of the available sequencing data, since much of the aligned sequence mapped to introns. There is also a distinct value in using samples from different tissues. Blood samples are informative in their own right, but comparing skin punch samples between SSc patients and unaffected controls reveals different gene sets more directly related to the ongoing molecular pathology.

The predominant signal in PBMCs was for type I interferon signaling, with enrichment for targets of IRF-5 and IRF-9. M1-polarized macrophages are known to have high *IRF5* expression (25). We observed that *CD86*, another marker of M1 macrophages, was increased in SSc PBMCs. Previous work has shown that a mix of monocytes with signs of M1 and M2 polarization in the blood is associated with interstitial lung disease in SSc patients (38). The lack of an increase of M2 markers does not necessarily exclude their presence. Bulk RNA-Seq is not ideal for identifying cell populations, and the question of macrophage fraction (and activation state) in SSc PBMCs would be better answered with single-cell RNA-Seq, flow cytometry, or mass cytometry.

The data from the analysis of skin samples provided an even more informative perspective. The most significantly different gene in the entire analysis was *SPAG17*, which has not traditionally been a top dysregulated gene in SSc transcriptome studies. Genes are often named for the tissue in which they are first discovered, which may or may not be the only tissue they are expressed in or even the tissue with the highest expression. *SPAG17* is a central pair protein that is critical in the formation of primary cilia, and its knockout is lethal in neonatal mice (39). As suggested by the name, alterations in *SPAG17* can lead to infertility in mouse models and for humans with certain rare missense

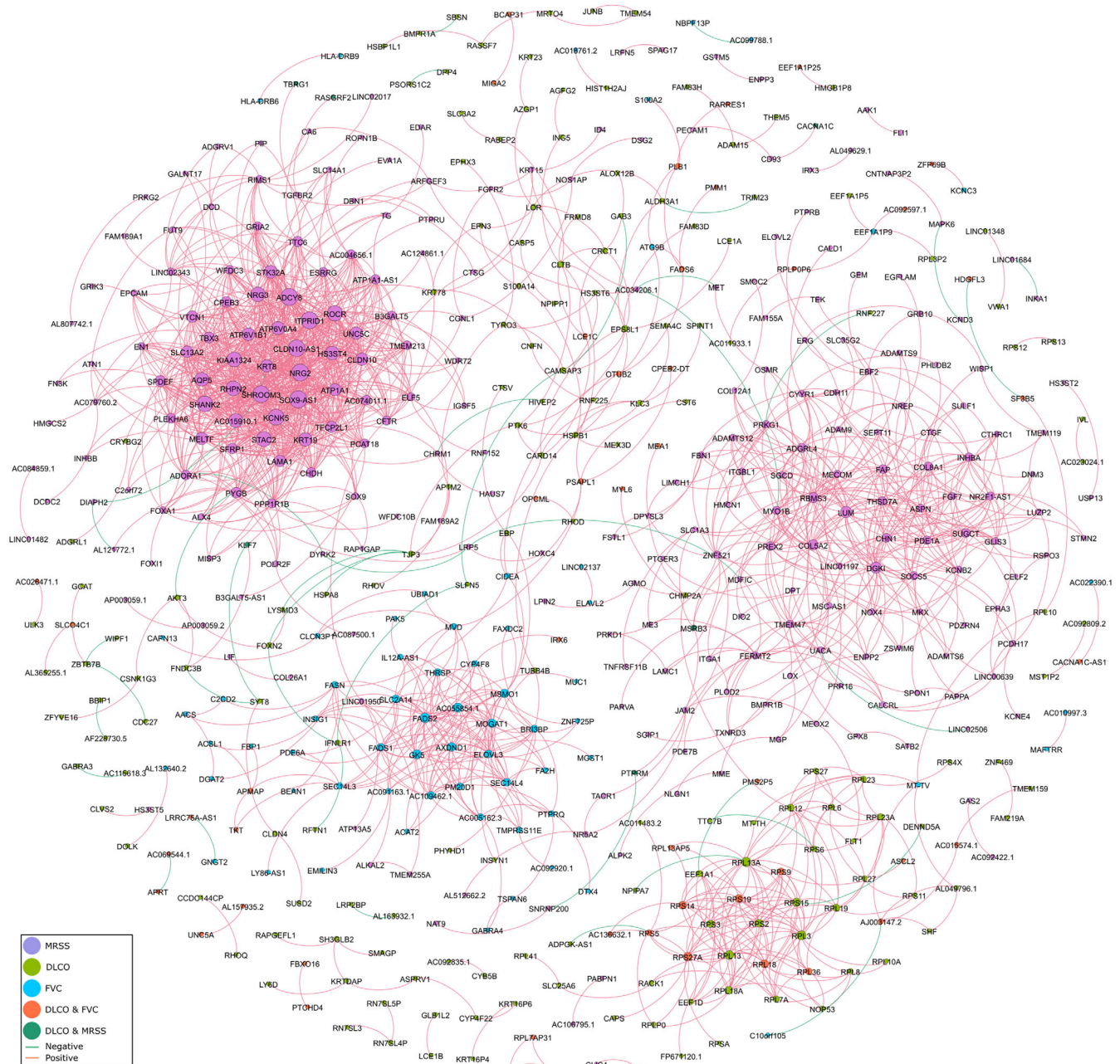


Figure 4. Network diagram of genes, particularly *SOX9* locus genes, most highly connected with at least 1 of the indicated clinical traits in systemic sclerosis (SSc) skin. Each node is an individual gene, sized by weighted degree and color-coded according to the trait association. The edges between nodes are color-coded to indicate whether the gene–gene correlation is positive or negative, with a minimum cutoff of 0.80. Some genes correlated with fibrosis formed a relatively separate subnetwork from those associated with lung function or both DLCO and fibrosis. The most connected genes in this subnetwork included *SOX9-AS1* and *ROCR*, which are both noncoding and located at the *SOX9* locus. The overlap of correlations between fibrosis and lung function was primarily ribosomal proteins. A separate subnetwork of the MRSS-correlated genes was enriched for matrix proteins, such as *COL5A2* and *COL8A1*. MRSS = modified Rodnan skin thickness score; DLCO = diffusing capacity for carbon monoxide; FVC = forced vital capacity.

variants (28,40). But it is important to bear in mind that this gene has critical functions beyond sperm motility since it is part of the primary cilia. Missense changes in *SPAG17* can cause abnormal bone length (29,41). Common variants in *SPAG17* are associated with body length in early life and height in adulthood (42,43). Novel

mutations and rare variants in components of the primary cilia can lead to primary ciliary dyskinesia (PCD). The most common effects are in the ears (chronic ear infections, hearing loss), sinuses (chronic sinus congestion), and lungs (recurrent pneumonia, chronic cough). Rare *SPAG17* variants can lead to a PCD-like

phenotype in mice and have been shown to cause human PCD as well (44,45). The PCD phenotypes are largely driven by the altered ability of the cilia to beat. In the skin of patients with SSc, a defect of beating cilia does not make the most sense. Nonmotile primary cilia are involved in signaling. One potential hypothesis is that primary cilia have an antifibrotic signaling role. The reduced expression could then lead to increased profibrotic signaling. Yet to be elucidated are the questions of whether mouse *Spag17* hypomorphs have increased fibrosis susceptibility, which cells in the skin are affected by reduced *SPAG17* expression, and why the *SPAG17* expression is decreased in the first place (i.e., whether it is a primary or secondary effect). One possibility is that *SPAG17* is lost in the transition from fibroblast to myofibroblast. Further research will be required to dissect these possibilities, particularly since the mouse germline knockout is lethal in neonatal mice.

We detected decreased expression of *LGR5* in the skin samples of SSc patients. The recent finding that *LGR5* is a marker for mouse intestinal villi tip telocytes begs the question of whether it is a marker of skin telocytes. The intestinal tip telocytes had increased expression of *Wnt5a* compared to the intestinal crypt telocytes, suggesting that noncanonical Wnt signaling is important in those cells (30). Skin telocytes are known to form multiple contacts to the extracellular matrix and other cells, such as adipose cells and fibroblasts (46). One possible function of these interconnections is to provide support for the other cells within the skin matrix. However, it is also possible that these cells are critical for the transduction of signals within the skin, and therefore may play a direct role in the evolution of fibrosis in the setting of SSc.

The skin of SSc patients had enrichment for pathways related to classical (antibody-mediated) complement activation. There is a growing body of evidence that complement activation and subsequent damage play a role in SSc endothelial damage. The terminal effector of complement damage, the membrane attack complex, has been observed in the small vessels of affected SSc skin and the muscle endothelium of patients with SSc-associated myositis (33,47). This indicates that local tissue damage, regardless of how it is triggered, may be complement-mediated. This possibility is perhaps even more evident in scleroderma renal crisis (SRC), which is characterized by a sudden onset of severe hypertension and acute renal failure. The kidneys of some individuals with SRC show deposition of complement C3b in renal arterioles (48,49). Complement deposition without substantial inflammation and the presence of thrombotic microangiopathy is also a hallmark of atypical hemolytic uremic syndrome (aHUS). Familial aHUS is often caused by the aberrant regulation of complement activation, particularly via genetic variants in complement factor H (50). The first-line therapy for aHUS is eculizumab, a monoclonal antibody to C5 (51). There is some evidence that eculizumab might also be effective for the treatment of SRC (52,53). However, this still leaves unanswered the question of whether endothelial complement activation is a major driver of vasculopathy in the skin of SSc patients.

The network analysis of PBMCs and skin transcriptomes with skin fibrosis and lung function parameters demonstrated that both tissues are informative for different traits, opening the possibility of the development of minimally invasive, quantitative biomarkers of disease activity. This would be a boon in clinical trials, particularly if observable parameters, such as the MRSS, do not tell the whole story regarding internal disease progression. Given the relatively small number of samples, further study is warranted to validate these findings. A particularly interesting facet of the clinical trait correlation in our study is the suggestion that *SOX9* is a critical player in fibrosis. Expression of the *ROCR* and *SOX9-AS1* noncoding RNAs, as well as *SOX9* itself, was significantly correlated with fibrosis in the skin of SSc patients. Importantly, *SOX9-AS1* and *ROCR* were 2 of the most highly interconnected genes in the SSc skin gene-gene coexpression network, suggesting that they have a key role in mediating the progression of fibrosis. Both are thought to help increase *SOX9* levels, perhaps via noncanonical transforming growth factor β signaling through Wnt/ β -catenin (54,55). The exact mechanism is not well defined. We previously demonstrated that blocking Wnt/ β -catenin signaling with C-82 restored subdermal adipogenesis in patients with SSc (56). However, since these are noncoding RNAs, it is currently unclear whether their effect is primarily through a role in regulating *SOX9* or through an alternative mechanism unrelated to *SOX9*. In particular, noncoding RNAs also act as linkers between DNA and protein. One such example is the *HOTAIR* noncoding RNA that mediates repression of some *HOX* loci by recruiting complexes to repress chromatin in those regions (57,58). Further investigation into the role and mechanism of action of *SPAG17* in profibrotic signaling and a better understanding of the roles of *ROCR* and *SOX9-AS1* in the skin are intriguing areas for future research.

AUTHOR CONTRIBUTIONS

All authors were involved in drafting the article or revising it critically for important intellectual content, and all authors approved the final version to be published. Dr. Roberson had full access to all of the data in the study and takes responsibility for the integrity of the data and the accuracy of the data analysis.

Study conception and design. Roberson, Atkinson, Varga.

Acquisition of data. Roberson, Carns, Cao, Aren, Goldberg, Korman, Varga.

Analysis and interpretation of data. Roberson, Morales-Heil.

REFERENCES

1. Van den Hoogen F, Khanna D, Fransen J, et al. 2013 classification criteria for systemic sclerosis: an American College of Rheumatology/European League against Rheumatism collaborative initiative. *Arthritis Rheum* 2013;65:2737–47.
2. Allanore Y, Simms R, Distler O, et al. Systemic sclerosis [review]. *Nat Rev Dis Primers* 2015;1:15002.
3. Varga J, Roberson ED. Genomic advances in systemic sclerosis: it's time for precision. *Arthritis Rheumatol* 2015;67:2801–5.
4. Derrett-Smith EC, Martyanov V, Chighizola CB, et al. Limited cutaneous systemic sclerosis skin demonstrates distinct molecular subsets

- separated by a cardiovascular development gene expression signature. *Arthritis Res Ther* 2017;19:156.
5. Assassi S, Wang X, Chen G, et al. Myeloablation followed by autologous stem cell transplantation normalises systemic sclerosis molecular signatures. *Ann Rheum Dis* 2019;78:1371–8.
 6. Beretta L, Barturen G, Vigone B, et al. Genome-wide whole blood transcriptome profiling in a large European cohort of systemic sclerosis patients. *Annals Rheum Dis* 2020;79:1218–26.
 7. Brkic Z, van Bon L, Cossu M, et al. The interferon type I signature is present in systemic sclerosis before overt fibrosis and might contribute to its pathogenesis through high BAFF gene expression and high collagen synthesis. *Ann Rheum Dis* 2016;75:1567–73.
 8. Higgs BW, Liu Z, White B, et al. Patients with systemic lupus erythematosus, myositis, rheumatoid arthritis and scleroderma share activation of a common type I interferon pathway. *Ann Rheum Dis* 2011;70:2029–36.
 9. Pendergrass SA, Lemaire R, Francis IP, et al. Intrinsic gene expression subsets of diffuse cutaneous systemic sclerosis are stable in serial skin biopsies. *J Invest Dermatol* 2012;132:1363–73.
 10. Skaug B, Khanna D, Swindell WR, et al. Global skin gene expression analysis of early diffuse cutaneous systemic sclerosis shows a prominent innate and adaptive inflammatory profile. *Ann Rheum Dis* 2020;79:379–86.
 11. Assassi S, Swindell WR, Wu M, et al. Dissecting the heterogeneity of skin gene expression patterns in systemic sclerosis. *Arthritis Rheumatol* 2015;67:3016–26.
 12. Apostolidis SA, Stifano G, Tabib T, et al. Single cell RNA sequencing identifies HSPG2 and APLNR as markers of endothelial cell injury in systemic sclerosis skin. *Front Immunol* 2018;9:2191.
 13. Karimizadeh E, Sharifi-Zarchi A, Nikaein H, et al. Analysis of gene expression profiles and protein-protein interaction networks in multiple tissues of systemic sclerosis. *BMC Med Genomics* 2019;12:199.
 14. Hinchcliff M, Huang CC, Wood TA, et al. Molecular signatures in skin associated with clinical improvement during mycophenolate treatment in systemic sclerosis. *J Invest Dermatol* 2013;133:1979–89.
 15. Johnson ME, Mahoney JM, Taroni J, et al. Experimentally-derived fibroblast gene signatures identify molecular pathways associated with distinct subsets of systemic sclerosis patients in three independent cohorts. *PLoS One* 2015;10:e0114017.
 16. Richardson C, Agrawal R, Lee J, et al. Esophageal dilatation and interstitial lung disease in systemic sclerosis: a cross-sectional study. *Semin Arthritis Rheum* 2016;46:109–14.
 17. Martin M. Cutadapt removes adapter sequences from high-throughput sequencing reads. *EMBnet J* 2011;17:10–2.
 18. Dobin A, Davis CA, Schlesinger F, et al. STAR: ultrafast universal RNA-seq aligner. *Bioinformatics* 2013;29:15–21.
 19. Liao Y, Smyth GK, Shi W. featureCounts: an efficient general purpose program for assigning sequence reads to genomic features. *Bioinformatics* 2014;30:923–30.
 20. Langfelder P, Horvath S. WGCNA: an R package for weighted correlation network analysis. *BMC Bioinformatics* 2008;9:559.
 21. Love MI, Huber W, Anders S. Moderated estimation of fold change and dispersion for RNA-seq data with DESeq2. *Genome Biol* 2014;15:550.
 22. Raudvere U, Kolberg L, Kuzmin I, et al. g:Profiler: a web server for functional enrichment analysis and conversions of gene lists (2019 update). *Nucleic Acids Res* 2019;47:W191–8.
 23. Fingerlin TE, Murphy E, Zhang W, et al. Genome-wide association study identifies multiple susceptibility loci for pulmonary fibrosis. *Nat Genet* 2013;45:613–20.
 24. Zhang Y, Wang S, Wang C, et al. High expression of FAM13A was associated with increasing the liver cirrhosis risk. *Mol Genet Genomic Med* 2019;7:e543.
 25. Krausgruber T, Blazek K, Smallie T, et al. IRF5 promotes inflammatory macrophage polarization and TH1-TH17 responses. *Nat Immunol* 2011;12:231–8.
 26. Duan H, Fleming J, Pritchard DK, et al. Combined analysis of monocyte and lymphocyte messenger RNA expression with serum protein profiles in patients with scleroderma. *Arthritis Rheum* 2008;58:1465–74.
 27. Assassi S, Mayes MD, Arnett FC, et al. Systemic sclerosis and lupus: points in an interferon-mediated continuum. *Arthritis Rheum* 2010;62:589–98.
 28. Kazarian E, Son H, Sapao P, et al. SPAG17 is required for male germ cell differentiation and fertility. *Int J Mol Sci* 2018;19:1252.
 29. Teves ME, Sundaresan G, Cohen DJ, et al. Spag17 deficiency results in skeletal malformations and bone abnormalities. *PLoS One* 2015;10:e0125936.
 30. Bahar Halpern K, Massalha H, Zwick RK, et al. Lgr5+ telocytes are a signaling source at the intestinal villus tip. *Nat Commun* 2020;11:1936.
 31. Manetti M, Rosa I, Messerini L, et al. A loss of telocytes accompanies fibrosis of multiple organs in systemic sclerosis. *J Cell Mol Med* 2014;18:253–62.
 32. Manetti M, Guiducci S, Ruffo M, et al. Evidence for progressive reduction and loss of telocytes in the dermal cellular network of systemic sclerosis. *J Cell Mol Med* 2013;17:482–96.
 33. Scambi C, Ugolini S, Jokiranta TS, et al. The local complement activation on vascular bed of patients with systemic sclerosis: a hypothesis-generating study. *PLoS One* 2015;10:e0114856.
 34. Farina G, Lafyatis D, Lemaire R, et al. A four-gene biomarker predicts skin disease in patients with diffuse cutaneous systemic sclerosis. *Arthritis Rheum* 2010;62:580–8.
 35. Christmann RB, Sampaio-Barros P, Stifano G, et al. Association of interferon- and transforming growth factor β -regulated genes and macrophage activation with systemic sclerosis-related progressive lung fibrosis. *Arthritis Rheumatol* 2014;66:714–25.
 36. Rice LM, Ziemek J, Stratton EA, et al. A longitudinal biomarker for the extent of skin disease in patients with diffuse cutaneous systemic sclerosis. *Arthritis Rheumatol* 2015;67:3004–15.
 37. Kim YH, Lee JR, Hahn MJ. Regulation of inflammatory gene expression in macrophages by epithelial-stromal interaction 1 (Epsti1). *Biochem Biophys Res Commun* 2018;496:778–83.
 38. Trombetta AC, Soldano S, Contini P, et al. A circulating cell population showing both M1 and M2 monocyte/macrophage surface markers characterizes systemic sclerosis patients with lung involvement. *Respir Res* 2018;19:186.
 39. Teves ME, Zhang Z, Costanzo RM, et al. Sperm-associated antigen-17 gene is essential for motile cilia function and neonatal survival. *Am J Respir Cell Mol Biol* 2013;48:765–72.
 40. Xu X, Sha YW, Mei LB, et al. A familial study of twins with severe asthenozoospermia identified a homozygous SPAG17 mutation by whole-exome sequencing. *Clin Genet* 2018;93:345–9.
 41. Cordova-Fletes C, Becerra-Solano LE, Rangel-Sosa MM, et al. Uncommon runs of homozygosity disclose homozygous missense mutations in two ciliopathy-related genes (SPAG17 and WDR35) in a patient with multiple brain and skeletal anomalies. *Eur J Med Genet* 2018;61:161–7.
 42. Van der Valk RJ, Kreiner-Moller E, Kooijman MN, et al. A novel common variant in DCST2 is associated with length in early life and height in adulthood. *Hum Mol Genet* 2015;24:1155–68.
 43. Kim JJ, Lee HI, Park T, et al. Identification of 15 loci influencing height in a Korean population. *J Hum Genet* 2010;55:27–31.
 44. Abdelhamed Z, Lukacs M, Cindric S, et al. A novel hypomorphic allele of Spag17 causes primary ciliary dyskinesia phenotypes in mice. *Dis Model Mech* 2020;13:dmm045344.

45. Andjelkovic M, Minic P, Vreca M, et al. Genomic profiling supports the diagnosis of primary ciliary dyskinesia and reveals novel candidate genes and genetic variants. *PLoS One* 2018;13:e0205422.
46. Rusu MC, Mirancea N, Manoiu VS, et al. Skin telocytes. *Ann Anat* 2012;194:359–67.
47. Corallo C, Cutolo M, Volpi N, et al. Histopathological findings in systemic sclerosis-related myopathy: fibrosis and microangiopathy with lack of cellular inflammation. *Ther Adv Musculoskelet Dis* 2017;9:3–10.
48. Okroj M, Johansson M, Saxne T, et al. Analysis of complement biomarkers in systemic sclerosis indicates a distinct pattern in scleroderma renal crisis. *Arthritis Res Ther* 2016;18:267.
49. Perez NA, Morales ML, Sanchez RS, et al. Endothelial lesion and complement activation in patients with Scleroderma Renal Crisis. *J Bras Nefrol* 2019;41:580–4.
50. Noris M, Caprioli J, Bresin E, et al. Relative role of genetic complement abnormalities in sporadic and familial aHUS and their impact on clinical phenotype. *Clin J Am Soc Nephrol* 2010;5:1844–59.
51. Cofiell R, Kukreja A, Bedard K, et al. Eculizumab reduces complement activation, inflammation, endothelial damage, thrombosis, and renal injury markers in aHUS. *Blood* 2015;125:3253–62.
52. Devresse A, Aydin S, Le Quintrec M, et al. Complement activation and effect of eculizumab in scleroderma renal crisis. *Medicine (Baltimore)* 2016;95:e4459.
53. Uriarte MH, Larrarte C, Rey LB. Scleroderma renal crisis debute with thrombotic microangiopathy: a successful case treated with eculizumab. *Case Rep Nephrol* 2018;2018:6051083.
54. Zhang W, Wu Y, Hou B, et al. A SOX9-AS1/miR-5590-3p/SOX9 positive feedback loop drives tumor growth and metastasis in hepatocellular carcinoma through the Wnt/ β -catenin pathway. *Mol Oncol* 2019;13:2194–210.
55. Barter MJ, Gomez R, Hyatt S, et al. The long non-coding RNA ROCR contributes to SOX9 expression and chondrogenic differentiation of human mesenchymal stem cells. *Development* 2017;144:4510–21.
56. Lafyatis R, Mantero JC, Gordon J, et al. Inhibition of β -catenin signaling in the skin rescues cutaneous adipogenesis in systemic sclerosis: a randomized, double-blind, placebo-controlled trial of C-82. *J Invest Dermatol* 2017;137:2473–83.
57. Tsai MC, Manor O, Wan Y, et al. Long noncoding RNA as modular scaffold of histone modification complexes. *Science* 2010;329:689–93.
58. Rinn JL, Kertesz M, Wang JK, et al. Functional demarcation of active and silent chromatin domains in human HOX loci by noncoding RNAs. *Cell* 2007;129:1311–23.